

## THERMOPHOTOVOLTAIC EFFICIENCY ENHANCEMENT THROUGH METAMATERIAL SELECTIVE EMITTERS

Nicole A. Pfister<sup>1</sup>, Dante F. DeMeo<sup>1</sup>, Corey M. Shemela<sup>2</sup>, and Thomas E. Vandervelde<sup>1</sup>

<sup>1</sup>Renewable Energy and Applied Photonics Labs, Department of Electrical and Computer Engineering, Tufts University, Medford, MA 02155

<sup>2</sup>Now at: Department of Computer and Electrical Engineering, University of Texas El Paso, 500 West University Avenue, El Paso, Texas 79968

**ABSTRACT:** Applying thermophotovoltaics (TPV) to present energy production technologies allows us to increase energy output while utilizing existing infrastructure by reclaiming the heat lost during the production process. In order to maximize the efficiency of these sources, the conversion efficiency of the TPV system needs to be optimized. Using metamaterials, we have created selective emitters that tailor the incident light spectrum to the band gap of specific diodes, offering the potential to reduce diode heating and increase efficiency. Usage of metals such as platinum and molybdenum makes the emitters able to withstand the high temperatures required to create ideal spectra for III-V cells. Simulations from CST Microwave Studio were used in the design process and testing of the emitters includes heat tests and SEM analysis.

**Keywords:** Thermophotovoltaic, Selective Emitter, Thermal Performance

### 1 INTRODUCTION

Due to recent advances in III-V semiconductor fabrication techniques, materials with narrow band gaps, such as InAs, can be used to make thermophotovoltaic (TPV) cells [1][2], [3], [4], [5], [6], [7][8] photovoltaic cells [9], [10] and photodetectors [11], [12], [13], [14], [15], [16], [17], [18], [19][20], [21], [22], [23][24], [25][26], [27][28], [29], [30] in the mid- to far-infrared frequency range. Spectral control measures, such as filters and selective emitters, are often implemented [2] to prevent excess thermalization in the cell.

Over the past decade, nanostructures have been used to generate novel optical interactions. These materials have since become known as metamaterials. Recently, negative refractive indices have been realized [31] and have led to research advances in the development of invisibility cloaks [32], perfect lenses [33], and other custom materials. In the past few years, the unique optical properties of metamaterials have been explored as a means for creating perfect absorbers and emitters of radiation [34].

Through impedance matching and the minimization of light transmission, narrowband perfect absorbers have been created [35]. According to Kirchoff's laws, the emission spectrum of a body is the same as the absorption spectrum; therefore, a perfect absorber can also be used as a perfect emitter. Such an emitter can be tailored to the band gap energy of a p-n junction as a way to more efficiently absorb light. The selective emitter minimizes extraneous device heating by rejecting light whose energy is too low to generate carriers or is too high and would generate significant phonon production via thermalization. This technology is of particular interest to the thermophotovoltaic (TPV) community. Application of a selective emitter to a TPV cell will increase the entire system efficiency, making TPV a more viable technology.

In order to maximize the power output, the selective emitter should be designed to operate at a temperature which aligns the peak of the blackbody spectrum at the wavelength of interest, as calculated by Planck's law.

### 2 BACKGROUND

Selective emitters with a large spectral peak in the infrared range have been fabricated previously [36]. However, the metal used in metamaterials like this tend to be gold [36] or aluminum [37]. The low melting points of these metals (660°C for aluminum, 1050°C for gold) become a problem when designing emitters for currently available TPV cells. To maximize the emitted power, a narrow band emitter should be heated to the temperature that places the maximum of the blackbody emission curve at the wavelength of interest, as seen in Figure 1. [38] Using Wien's displacement law (Eq. 1), we can calculate that temperature given a target peak wavelength,

$$\lambda_{\max} T = b \quad \text{Eq. 1}$$

where  $\lambda_{\max}$  is the peak wavelength, T is the blackbody temperature in Kelvin, and b is Wien's displacement constant, which is equal to  $2.898 \times 10^{-3} \text{ m}\cdot\text{K}$ . For example, an emitter for a GaSb TPV cell with a band gap of 0.7eV, corresponding to a  $1.77\mu\text{m}$  wavelength, would need to be at 1400°C for optimal performance. Metamaterials made of either gold or aluminum would degrade past the point of operation long before the optimal temperature was reached.

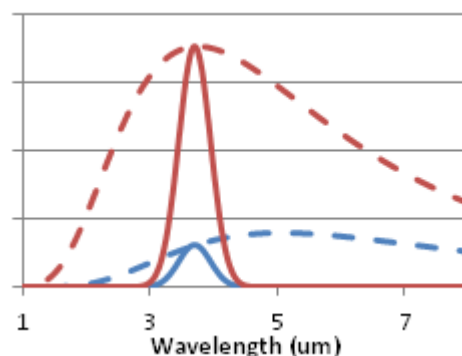


**Figure 1.** Comparison of produced power and bandwidth

for a blackbody (dashed lines) at 500°C (red) and 300°C (blue) and the power output of their respective selective emitters (solid lines) targeting a 3.7 $\mu\text{m}$  wavelength.

To create selective thermal emitters that can be coupled with available TPV cells, we utilized platinum and molybdenum as the basis for metamaterials targeted at different wavelengths. These metals were selected for their relatively high melting points; about 1700°C and 2600°C, respectively.

### 3 SIMULATION

#### 3.1 Method

Wien's displacement law was used to determine the peak wavelength of a blackbody at the temperatures of interest. At 500°C, this corresponded to 3.75 $\mu\text{m}$  (80 THz) and at 1000°C, the peak wavelength was at 2.28 $\mu\text{m}$  (131.7 THz). Platinum was used as the metal for a 500°C optimized selective emitter. From previous work[39], platinum nanostructures can degrade well below the melting point, so molybdenum was used as the metal for a 1000°C optimized selective emitter.

Simulations were performed using CST Microwave Studio, based on the models developed for previous work[39]. Materials characteristics such as conductivity and plasma frequency were based on Drude model calculations from Ordal et al.[40]

The designs were optimized based on several criteria. Most importantly, the selective absorption peak had to appear within 100nm of the target wavelength. Selectivity is also an important characteristic of these emitters, so the full-width, half-maximum (FWHM) was minimized as much as possible with the goal of being less than 50nm. Finally, the percentage of the impinging light that is absorbed at the target wavelength is directly proportional to the amount of light transmitted from the emitter when it is heated. Therefore, it was very important to maximize the absorption percentage to also maximize the power emitted in the desired band.

The procedure for optimization began with rough alignment of the absorption peak through manipulation of the metamaterial pattern dimensions and the size of the unit cell. The complexity of the pattern affected the FWHM of the peak with more complex designs resulting

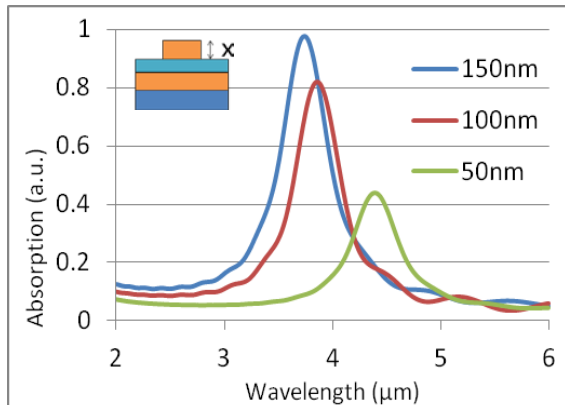


**Figure 2.** Simulation data for the 500°C emitter made from platinum with varying top layer thicknesses (see inset for side view of unit cell) of 50nm (green), 100nm (red), and 150nm (blue).

in a sharper peak. Therefore, crosses were selected as the basis for the patterns rather than simple rectangles or circles. More complex patterns were not feasible for the target wavelengths as the dimensions became smaller than the resolution of the electron beam lithography tool used in fabrication. Finally, absorption percentage was found to be dependent on the thickness of the patterned metal layer, as can be seen by the peak wavelength drift in Figures 2 and 3. By adjusting each of these aspects of the design, we were able to develop sharp, selective peaks with near unity absorption.

#### 3.2 Simulation Results

For the 500°C emitter, the metamaterial pattern consisted of a cross whose arms were 770nm by 150nm rectangles in a 1 $\mu\text{m}$  unit cell. This pattern was then repeated in a square lattice over the desired write-field. A top metal layer thickness of 150nm was found to provide the highest absorption rate, as shown by the simulation results in Figure 2. For the 1000°C emitter, the pattern consisted of a cross with 450nm by 100nm arms on an 800nm unit cell. Again, this pattern was repeated over the desired write-field. The ideal top metal thickness for molybdenum was found to be 30nm. Both designs were reproduced with the addition of a 10nm alumina capping layer. Simulated spectra for each design can be seen in Figures 2 and 3.

Several thicknesses were simulated for both platinum (Figure 2) and molybdenum (Figure 3). Along with varied absorption, the changing layer thickness introduced a fair amount of peak shift. Had those thicknesses been desirable, the pattern dimensions would have had to be adjusted to shift the peak back to the target wavelength.

### 4 FABRICATION

#### 4.1 Method

Two-inch, single side polished sapphire wafers were used as the main substrate of the MM emitters. A 100nm grounding plane of metal was deposited on the sapphire using electron beam evaporation with a 20nm layer of alumina deposited on top of that using atomic layer deposition (ALD).

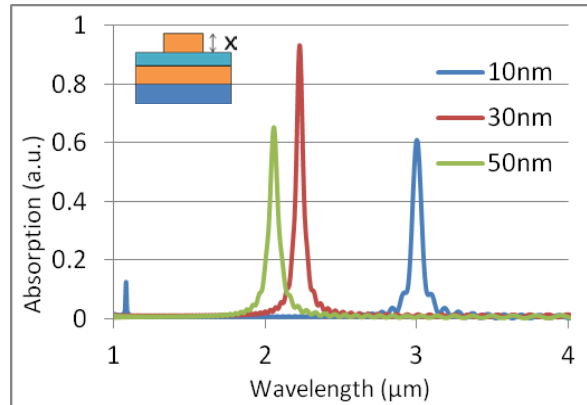


**Figure 3.** Simulation data for the 1000°C emitter made from molybdenum with varying top layer thicknesses (see inset for side view of unit cell) of 50nm (green), 30nm (red), and 10nm (blue).

After dicing into smaller chips, electron beam lithography was used to expose the pattern into PMMA C6 resist. The metamaterial metal was then deposited via PVD, followed by liftoff in acetone. Samples with an additional capping layer of alumina were also fabricated to guard against oxidation and surface effects.

#### 4.2 Fabrication Results

The emitters were imaged via SEM to ensure close match with the simulations. These images can be seen in Figures 4 and 5. They show close match to the desired pattern dimension, with some differences due to the electron beam dosage used in the fabrication process. Further optimization of electron beam write procedures are expected to mitigate the difference between the designed pattern and fabricated pattern. Absorption data via Fourier transform infrared spectroscopy will be forthcoming.

#### 5 CONCLUSION

Selective thermal emitters made of platinum and molybdenum were simulated and fabricated. Time domain simulations using material properties from the Drude model was used to optimize the metamaterial pattern dimensions and layer thicknesses. The optimization process included reducing the FWHM and increasing the percentage of light absorbed at the target wavelength. By optimizing and tailoring the selective thermal emitter spectrum to a specific band gap, we can increase the efficiency of thermophotovoltaic cells.

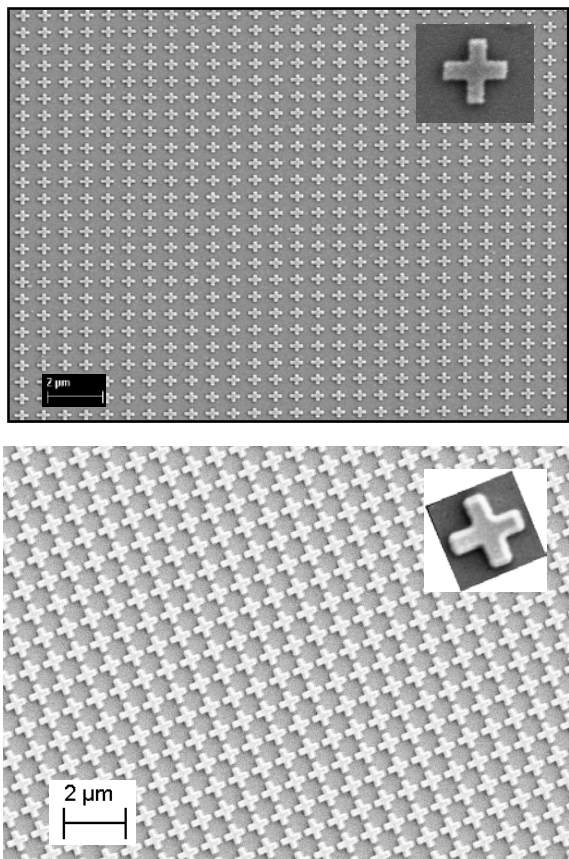


**Figure 5.** SEM image of the molybdenum (top) and platinum (bottom) emitter pattern without a capping layer. The inset shows the unit cell that was repeated over the write field.

#### 6 REFERENCES

- [1] D. DeMeo, A. Licht, and T. Vandervelde, "Thermophotovoltaics: An alternative to and potential partner with rectenna energy harvesters," in *Rectenna Solar Cells*, 2013.
- [2] C. M. Shemelya and T. E. Vandervelde, "Comparison of Photonic-Crystal-Enhanced Thermophotovoltaic Devices With and Without a Resonant Cavity," *Journal of Electronic Materials*, vol. 41, no. 5, pp. 928–934, 2012.
- [3] D. F. DeMeo and T. E. Vandervelde, "Cryogenic thermal simulator for testing low temperature thermophotovoltaic cells," *J. Vac. Sci. Technol. B*, vol. 29, 2011.
- [4] C. M. Shemelya and T. E. Vandervelde, "Photonic Crystal Resonant Cavity for Thermophotovoltaic Applications," in *37th IEEE Photovoltaic Specialist Conference*, 2011.
- [5] D. F. DeMeo and T. E. Vandervelde, "Simulations of Gallium Antimonide (GaSb) p-B-n Thermophotovoltaic Cells," in *MRS Spring Meeting*, 2011, p. 1329.
- [6] C. Shemelya and T. E. Vandervelde, "Thermophotovoltaic Enhancement: 2D Photonic Crystals to Increase TPV Efficiencies," in *MRS Proceedings*, 2009, p. 1208.
- [7] D. F. DeMeo and T. E. Vandervelde, "Simulations of Indium Arsenide Antimonide (InAs<sub>0.91</sub>Sb<sub>0.09</sub>) Lattice Matched to GaSb Barrier-Based Thermophotovoltaic Cells," in *37th IEEE Photovoltaic Specialist Conference*, 2011.
- [8] C. M. Downs and T. E. Vandervelde, "Investigating Thallium Based Materials for Use in Multijunction Photovoltaics," in *37th IEEE Photovoltaic Specialist Conference*, 2011.
- [9] D. DeMeo, C. Shemelya, C. Downs, S. Magden, A. Licht, T. E. Vandervelde, C. Dhital, S. Wilson, T. Rotter, and G. Balakrishnan, "GaSb Thermophotovoltaic Cells Grown on GaAs Substrate Using the Interfacial Misfit Array Method," *Journal of Electronic Materials*.
- [10] C. M. Downs and T. E. Vandervelde, "Bridging the Multijunction Solar Cell Band-Gap Chasm Using GaTIP," *Applied Physics Letters*.
- [11] C. Downs and T. E. Vandervelde, "Progress in Infrared Photodetectors Since 2000 No Title," *Sensors*, vol. 13, pp. 5054–5098, 2013.
- [12] R. Rehm, M. Masur, J. Schmitz, V. Daumer, J. Niemasz, T. Vandervelde, D. DeMeo, W.

- Luppold, M. Wauro, A. Wörl, F. Rutz, R. Scheibner, J. Ziegler, and M. Walther, "InAs/GaSb Superlattice Infrared Detectors," *Infrared Physics & Technology*, 2012.
- [13] L. Fu, T. E. Vandervelde, and S. Krishna, "Quantum Dot Infrared Photodetectors," in *VLSI Microphotonics: Science, Technology and Application*, 2010.
- [14] R. Sheno, R. Attaluri, A. Siroya, J. Shao, Y. Sharma, A. Stintz, T. Vandervelde, and S. Krishna, "Low-strain InAs/InGaAs/GaAs quantum dots-in-a-well infrared photodetector," *Journal of Vacuum Science & Technology B*, vol. 26, no. 3, pp. 1136–1139, 2008.
- [15] J. Rosenberg, R. Sheno, T. Vandervelde, S. Krishna, and O. Painter, "A multispectral and polarization-selective surface-plasmon resonant midinfrared detector," *Applied Physics Letters*, vol. 95, no. 161101, 2009.
- [16] W.-Y. Jang, M. M. Hayat, J. S. Tyo, R. S. Attaluri, T. E. Vandervelde, Y. D. Sharma, R. Sheno, A. Stintz, E. R. Cantwell, S. C. Bender, S. J. Lee, S. K. Noh, and S. Krishna, "Demonstration of bias-controlled algorithmic tuning of quantum dots in a well (DWELL) midIR detectors," *IEEE Journal of Quantum Electronics*, vol. 45, no. 6, pp. 674–683, 2009.
- [17] T. E. Vandervelde, M. C. Lenz, E. Varley, A. Barve, J. Shao, R. V. Sheno, D. A. Ramirez, W. Jan, Y. D. Sharma, and S. Krishna, "Quantum dots-in-a-well focal plane arrays," *IEEE Journal of Quantum Electronics*, vol. 14, no. 4, pp. 1150–1161, 2008.
- [18] A. Barve, S. Shah, J. Shao, T. Vandervelde, R. Sheno, W. Jang, and S. Krishna, "Reduction in dark current using resonant tunneling barriers in quantum dots-in-a-well long wavelength infrared photodetector," *Applied Physics Letters*, vol. 93, no. 131115, 2008.
- [19] J. Rosenberg, R. V. Sheno, T. E. Vandervelde, S. Krishna, and O. Painter, "A multispectral and polarization-selective surface-plasmon resonant midinfrared detector," *Applied Physics Letters*, vol. 95, no. 16, p. 161101, 2009.
- [20] A. Barve, J. Shao, Y. Sharma, T. Vandervelde, K. Sankalp, S. Lee, S. Noh, and S. Krishna, "Resonant Tunneling Barriers in Quantum Dots-in-a-Well Infrared Photodetectors," *IEEE Journal of Quantum Electronics*, vol. 46, no. 7, pp. 1105–1114, 2012.
- [21] R. Sheno, J. Rosenberg, T. Vandervelde, O. Painter, and S. Krishna, "Multispectral quantum dots-in-a-well infrared detectors using plasmon assisted cavities," *IEEE Journal of Quantum Electronics*, vol. 46, no. 7, pp. 1051–1057, 2010.
- [22] J. R. Andrews, S. R. Restaino, T. E. Vandervelde, J. S. Brown, Y. D. Sharma, S. J. Lee, S. W. Teare, A. Reisinger, M. Sundaram, and S. Krishna, "Comparison of long-wave infrared quantum-dots-in-a-well and quantum-well focal plane arrays," *IEEE Transactions on Electron Devices*, vol. 56, no. 3, pp. 512–516, 2009.
- [23] P. Vines, C. Tan, J. David, R. Attaluri, T. Vandervelde, and S. Krishna, "Multiple stack quantum dot infrared photodetectors," in *SPIE, Electro-Opt. Infrared Syst.: Technol. Appl*, 2008, p. 7113.
- [24] P. Vines, C. H. Tan, J. P. David, R. S. Attaluri, T. E. Vandervelde, S. Krishna, W.-Y. Jang, and M. M. Hayat, "Versatile spectral imaging with an algorithm-based spectrometer using highly tuneable quantum dot infrared photodetectors," *IEEE Journal of Quantum Electronics*, vol. 47, no. 2, pp. 190–197, 2011.
- [25] P. Vines, C. Tan, J. David, R. Attaluri, T. Vandervelde, S. Krishna, W.-Y. Jang, and M. Hayat, "Quantum dot infrared photodetectors with highly tunable spectral response for an algorithm-based spectrometer," in *Proceedings of SPIE*, 2010, p. 7660.
- [26] T. Vandervelde and S. Krishna, "Progress and Prospects for Quantum Dots in a Well Infrared Photodetectors," *Journal of Nanoscience and Nanotechnology*, vol. 10, no. 3, pp. 1450–1460, 2010.
- [27] J. Shao, T. Vandervelde, W. Jang, A. Stintz, and S. Krishna, "High operating temperature InAs quantum dot infrared photodetector via selective capping techniques," in *IEEE Conference on Nanotechnology*, 2008, pp. 112–115.
- [28] R. Sheno, J. Hou, Y. Sharma, J. Shao, T. Vandervelde, and S. Krishna, "Low strain quantum dots in a double well infrared detectors," in *Infrared Spaceborne Remote Sensing and Instrumentation XVI SPIE*, 2008, p. 7082.
- [29] J. Shao, T. Vandervelde, A. Barve, W. Jang, A. Stintz, and S. Krishna, "Enhanced normal incidence photocurrent in quantum dot infrared photodetectors," *Journal of Vacuum Science & Technology B*, vol. 29, p. 03C123, 2011.
- [30] C. Downs and T. E. Vandervelde, "Progress in Infrared Photodetectors Since 2000 No Title," *Sensors*, vol. 13, pp. 5054–5098, 2013.
- [31] D. R. Smith, W. J. Padilla, D. C. Vier, S. C. Nemat-Nasser, and S. Schultz, "Composite Medium with Simultaneously Negative Permeability and Permittivity," *Phys. Rev. Lett.*, vol. 84, pp. 4184–4187, 2000.

- [32] D. Schurig, J. J. Mock, B. J. Justice, S. A. Cummer, J. B. Pendry, A. F. Starr, and D. R. Smith, "Metamaterial electromagnetic cloak at microwave frequencies.," *Science (New York, N.Y.)*, vol. 314, no. 5801, pp. 977–80, Nov. 2006.
- [33] N. Fang and X. Zhang, "Imaging properties of a metamaterial superlens," *Applied Physics Letters*, vol. 82, no. 2, p. 161, 2003.
- [34] C. Wu, B. Neuner III, J. John, A. Milder, B. Zollars, S. Savoy, and G. Shvets, "Metamaterial-based integrated plasmonic absorber/emitter for solar thermo-photovoltaic systems," *Journal of Optics*, vol. 14, no. 2, p. 024005, Feb. 2012.
- [35] N. Landy, S. Sajuyigbe, J. Mock, D. Smith, and W. Padilla, "Perfect Metamaterial Absorber," *Physical Review Letters*, vol. 100, no. 20, p. 207402, May 2008.
- [36] X. Liu, T. Tyler, T. Starr, A. Starr, N. Jokerst, and W. Padilla, "Taming the Blackbody with Infrared Metamaterials as Selective Thermal Emitters," *Physical Review Letters*, vol. 107, no. 4, pp. 4–7, Jul. 2011.
- [37] F. Alves, B. Kearney, D. Grbovic, and G. Karunasiri, "Narrowband terahertz emitters using metamaterial films.," *Optics express*, vol. 20, no. 19, pp. 21025–32, Sep. 2012.
- [38] M. Planck, "Ueber das Gesetz der Energieverteilung im Normalspectrum," *Annalen der Physik*, vol. 309, no. 3, pp. 553–563, 1901.
- [39] C. M. Shemelya, "Photonics : Photodiodes and Metamaterials for Thermophotovoltaics and Photodetection Applications," Tufts University, 2013.
- [40] M. a Ordal, L. L. Long, R. J. Bell, S. E. Bell, R. R. Bell, R. W. Alexander, and C. a Ward, "Optical properties of the metals Al, Co, Cu, Au, Fe, Pb, Ni, Pd, Pt, Ag, Ti, and W in the infrared and far infrared.," *Applied optics*, vol. 22, no. 7, pp. 1099–20, Apr. 1983.